Transversal Stiffness and Young's Modulus of Single Fibers from Rat Soleus Muscle Probed by Atomic Force Microscopy

Irina V. Ogneva,[†*] Dmitry V. Lebedev,[‡] and Boris S. Shenkman[†]
[†]State Scientific Center of Russian Federation Institute for Biomedical Problems of Russian Academy of Sciences, Moscow, Russia; and [‡]Petersburg Nuclear Physics Institute, Gatchina, Russia

ABSTRACT The structural integrity of striated muscle is determined by extra-sarcomere cytoskeleton that includes structures that connect the Z-disks and M-bands of a sarcomere to sarcomeres of neighbor myofibrils or to sarcolemma. Mechanical properties of these structures are not well characterized. The surface structure and transversal stiffness of single fibers from soleus muscle of the rat were studied with atomic force microscopy in liquid. We identified surface regions that correspond to projections of the Z-disks, M-bands, and structures between them. Transversal stiffness of the fibers was measured in each of these three regions. The stiffness was higher in the Z-disk regions, minimal between the Z-disks and the M-bands, and intermediate in the M-band regions. The stiffness increased twofold when relaxed fibers were maximally activated with calcium and threefold when they were transferred to rigor (ATP-free) solution. Transversal stiffness of fibers heavily treated with Triton X-100 was about twice higher than that of the permeabilized ones, however, its regional difference and the dependence on physiological state of the fiber remained the same. The data may be useful for understanding mechanics of muscle fibers when it is subjected to both axial and transversal strain and stress.

INTRODUCTION

Muscle fiber can be considered as a compound mechanical system where the mechanical stress is transduced not only in the axial, but also in the lateral direction (1). The contractile apparatus is formed by myofibrils that are elongated in the fiber axis and occupy most of its volume. Mechanical properties of the whole fiber are thus determined by structural and functional interaction of the three mechanically different compartments: myofibrils, extra sarcomeric cytoskeleton, and sarcolemma.

One can expect that changes in the mechanical properties of each of these three compartments would result in changes in the transversal stiffness of a muscle fiber. The difference in transversal fiber stiffness in the regions that correspond to the Z-disks and M-bands of sarcomeres is of particular interest because some proteins in the extra sarcomere structures perpendicular to the fiber axis in the regions of the Z-disks (costameres) participate in signal pathways (2,3). Mechanical properties of the M-band regions are also important as the titin kinase domain that serves as a mechanosensor is localized in the M-bands (4,5). One could furthermore assume that the lateral mechanical elements of the extra sacomeric cytoskeleton that connect myofibrils laterally are important for keeping uniform sarcomere length during activation. Uniform sarcomere length is necessary for maximal force generation. Thus, to understand the properties of a whole fiber on a sarcomere level there is a need for data on lateral mechanical properties.

Mathur et al. (6) have obtained first data of mechanical characteristics of intact cell of skeletal and cardiac muscles using atomic force microscopy (AFM) in liquid. They found that the transversal Young modulus is 100.3 ± 10.7 kPa for cardiac and 24.7 ± 3.5 kPa for skeletal muscles. Cardiac muscles are stiffer than skeletal muscles, and offer better resistance to deformation. This is probably due to their permanent rhythmic contractions. Defranchi et al. (7) studied structure and transversal stiffness of sarcolemma in fully differentiated muscle fibers at different conditions. They used muscle fibers of the mice of line CD1 either in culture or air-dried. They estimated the Young's modulus to be 61 ± 5 kPa.

The 2.5 times difference between the figures obtained by Defranchi et al. (7) and Mathur et al. (6) may result from the difference in preparations: fully differentiated in Defranchi et al. (7) and myoblasts in Defranchi et al. (6). Collinsworth et al. (8) studied the mechanical properties of muscle fibers during their differentiation. They found that the Young modulus increases sharply on day 8 of the differentiation from 11.5 ± 1.3 kPa to 45.3 ± 4.0 kPa on the days 8–10 of differentiation. The difference indicates nonuniform dynamics of expression of different proteins that define transversal stiffness during ontogenesis. We could not find any published data concerning the difference in Young modulus between different regions along a sarcomere.

The aim of this study was to examine the lateral mechanical properties of different parts of isolated muscle fibers in relaxed, calcium-activated, and rigor states in the projections of the Z-disks, M-bands, and regions between them. We also compared the results of AFM measurements of transversal stiffness of muscle fibers in saline solution with those obtained in wet air.

Submitted June 16, 2009, and accepted for publication October 21, 2009.

*Correspondence: iogneva@yandex.ru

Editor: K. W. Ranatunga.

0006-3495/10/02/0418/7 $2.00

doi: 10.1016/j.bpj.2009.10.028

MATERIALS AND METHODS

Sample preparation

Adult male Wistar rats ($n = 15$ animals) were raised at the animal house of State Scientific Center of Russian Federation Institute for Biomedical Problems of Russian Academy of Sciences to the age of 2 months under standard conditions. Animals received standard food and water. Animals were euthanized before experiments. All experimental procedures were approved by the Biomedical Ethics Committee of State Scientific Center of Russian Federation Institute for Biomedical Problems of Russian Academy of Sciences.

Entire soleus was extracted from the animal tendon to tendon, and subjected to chemical skinning to cause partial lysis of the cell membranes as described by Stevens et al. (9). The obtained muscle samples were stored at −20°C in a mixture of equal volumes of glycerol and relaxing solution *R*, containing 20 mM MOPS, 170 mM potassium propionate, 2.5 mM magnesium acetate, 5 mM K_2EGTA, and 2.5 mM ATP. On the day of the experiment the muscle was transferred to the relaxing solution *R* and single fibers were isolated from the muscle.

Triton-treated samples were obtained by incubation of isolated muscle fibers in Triton X-100 (final concentration 2% by volume) for 12 h at +4°C. The detergent concentration and the incubation time used during preparation ensured complete removal of the cell membrane while leaving the myofibrillar apparatus of the muscle fiber intact. The fibers were subsequently washed from the remaining detergent in solution *R* and prepared for AFM measurements following the same procedure as the permeabilized fibers.

For AFM in liquid, the ends of the fibers were attached to the bottom of the microscopy cell with Fluka shellac wax-free glue (Sigma, St. Louis, MO). Depending on the experiment series, the cell was filled with ether the relaxing solution *R*, activating solution *A* containing 20 mM MOPS, 172 mM potassium propionate, 2.38 mM magnesium acetate, 5 mM CaEGTA, 2.5 mM ATP (pCa 4.2), or rigor solution *Rg* of the same composition as solution *R* but without ATP. Because the ends of the fibers were fixed, the contractions in solution *A* were isometric.

For AFM measurements in air the fibers with their ends glued to glass were incubated in one of the solutions (*R*, *A*, or *Rg*). Then the solution was removed by suction (wet sample) and AFM measurements were carried out for 1–10 min.

All measurements were carried out at +12°C.

AFM

AFM is a useful tool for studying cell mechanics (6–8). It is based on mechanical interaction of a cantilever with the specimen surface. This approach allows one to visualize the specimen surface and to measure its mechanical properties. For stiffness measurement, force curves have been obtained: a cantilever whose stiffness was calibrated before an experiment was pressed against the surface. By measuring its deflection with an optical transducer both force and displacement of the cantilever have been estimated. Using measurements of cantilever displacement and deflection force-displacement diagram of the specimen have been calculated.

Measurements of transverse stiffness of both permeabilized and Triton-treated fibers were carried out using Solver-Bio atomic force microscope (NT-MDT, Moscow, Russia) equipped with SMENA AFM head mounted on Olympus XI inverted light microscope (Olympus Corporation, Tokyo, Japan). Silicon cantilevers were obtained from NT-MDT; the stiffness coefficient of each cantilever was corrected using its natural resonance frequency according to the procedure supplied by NT-MDT.

The surface scans of slightly wet fibers in air were obtained in semicontact mode using silicon cantilever with the length of 150 μm and the stiffness of 5–6 N/m. Force-distance curves were obtained in contact mode using cantilever with the length of 250 μm, tip cone angle of 22°, and the stiffness of 0.08–0.12 N/m. All AFM measurements in liquid were carried out in contact mode using soft contact cantilevers with the stiffness coefficient ~0.05 N/m. The depth of the surface scanning was ~1 nm to minimize surface deformation by the cantilever.

The surface scan was used to determine the length of the sarcomeres and to identify the Z-disk and M-band regions of the fiber (see Fig. 2). The fiber surface had a structure with axial period of 2.3–2.5 μm consisting of two regions. One region was 1.5–1.7 μm long and was attributed to the A-band with M-band in the middle. Another region, 0.7–0.9 μm long, probably corresponds to the I-band with Z-disk in the middle.

Force-distance curves were obtained by registering the dependency of the cantilever deflection on its position along vertical z axis perpendicular to the fiber axis. The applied force F_s (in N) was calculated using the formula

$$F_s = k_c \times \frac{I(z)}{a},$$

where $I(z)$ (in A) is the measured deflection current, z (in m) is indentation depth, a (in A/m) is the slope of the calibration curve registered on the bottom of a Perspex cell and k_c (in N/m) is the cantilever stiffness, that was estimated after the procedure specified by the AFM manufacturer (NT-MDT). A thousand data points have been obtained for each force curve. The true indentation depth h_s (in m) was calculated by the formula

$$h_s = z - \frac{F_s}{k_c}.$$

The transverse stiffness of the fiber k_s (in N/m) was calculated for the indentation depth $h_{s1} = 150$ nm:

$$k_s = \frac{F_{s1}}{h_{s1}},$$

where F_{s1} (in N) is applied force need to get a $h_{s1} = 150$ nm depth of cantilever penetration.

This depth has been chosen for excluding mechanical effect on deeper structures because the distance between sarcolemma and first superficial myofibril is at least 200 nm and in average 800–1000 nm as determined using electron microscopy (10).

To calculate Young modulus of the fiber, E_s, from the force curves we followed (11), we used Sneddon's modification of the Hertz model for the elastic indentation of a flat, soft sample by a stiff sphere that modeled the cantilever tip (12,13). The force-distance curves were fitted to the following formula yielding the Young modulus of the fiber (Fig. 1):

$$F_s = \frac{4E_s r_c^{\frac{1}{2}}}{3\left(1-\mu_s^2\right)} h_s^{\frac{3}{2}}, \quad (1)$$

where μ_s is the Poisson coefficient, taken to be 0.5 in approximation of incompressible cell (6,8,14,15). The curvature of the cantilever tip r_c was 10 nm.

Fit of the data to the solution of Hertz problem (11) (Fig. 1) yielded the best coefficient of significance of the approximation R^2 (~0.98) as compared to linear fit ($R^2 = 0.94$) (7) or parabola ($R^2 = 0.91$) (8).

Data were processed with fitting procedures written in MATLAB 6.5 (The MathWorks, Natick, MA). Standard Microsoft Excel procedures were used for statistical analysis. Unless stated otherwise the results are presented as mean ± SE.

RESULTS

Analysis of the surface of muscle fibers

The surface scan of the permeabilized muscle fibers in relaxed state shows protuberances (referred to here as ''humps'') both near the Z-disk and M-band projections (Fig. 2). The hump near the Z-disk is probably due to the presence of the costamere, submembrane structures between

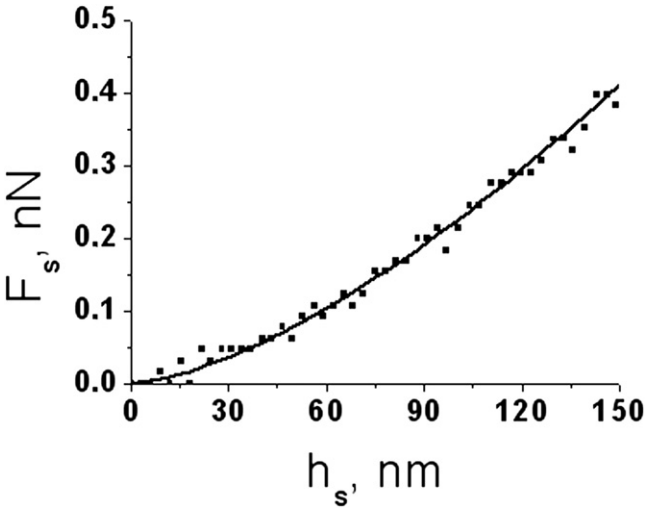

FIGURE 1 Sample force-distance curve obtained at Z-disk projection on relaxed permeabilized fiber, showing a typical dependency of the applied force on the depth of indentation. Squares show experimental points, line represents the least-square fit to Eq. 1 (Young's modulus 38.5 kPa, apparent transversal stiffness 2.72 pN/nm at 150 nm indentation).

the membrane and the contractile apparatus. A costamere-like structure that connects the M-band to sarcolemma probably exists near the M-band. Triton-treated fibers show smaller humps and similar heights near the Z-disks and M-bands (Fig. 3).

The sarcomere length in relaxed state measured as the distance between the neighboring Z-disk projections along the direction perpendicular to the Z-disks (Fig. 2) was 2.48 $\pm$ 0.03 μm ($n = 391$).

Transition from relaxed to rigor state had a marked effect on the fiber surface (Fig. 4). Some additional features became visible on the surface profile (Fig. 4 *B*) that may indicate a substantial reorganization of not only in the contractile apparatus but also of the extra sarcomeric cytoskeleton, especially in the projection of the Z-disks. Similar, although less pronounced changes in the fiber surface were observed in Ca-activated state. The average sarcomere length in the Ca-activated fibers was 2.42 $\pm$ 0.06 μm ($n = 402$).

Transversal stiffness of muscle fibers

Force-distance curves obtained on relaxed isolated muscle fibers show that the transverse stiffness was significantly higher for Triton-treated than for permeabilized fibers (Fig. 5). This difference was clear in the measurements taken at both M-band and Z-disk (or their projections in permeabilized fibers; Fig. 5, *B* and *C*, respectively), as well as between M-band and Z-disk (reflecting the stiffness of the sarcolemma in Triton-treated, and the costamere in permeabilized fibers; Fig. 5 *A*).

In all measurements, the transverse stiffness was the lowest in the area between the M-band and Z-disk, and the highest at Z-disk. In both permeabilized and Triton-treated

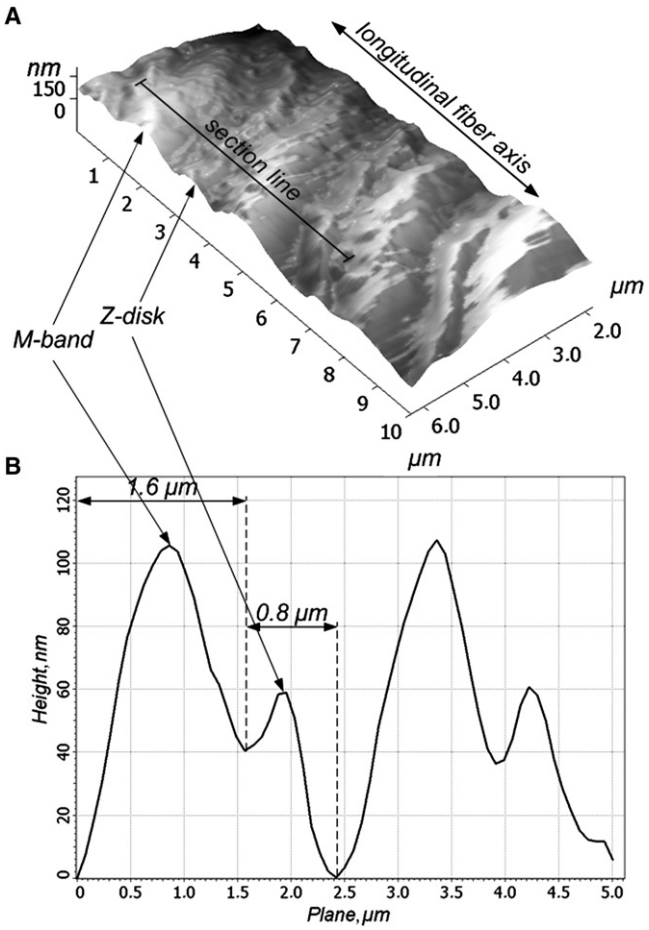

FIGURE 2 Three-dimensional AFM area scan (*A*) and a surface profile (*B*) along a section line shown in *A* of a permeabilized fiber from rat soleus muscle in relaxed state. There two kinds of humps on a surface profile. Those of ~1.6 μm in length correspond to the A-bands with the M-bands in the middle. Other humps (0.8 μm) probably correspond to the I-bands with the Z-disks in the middle.

fibers the highest transverse stiffness was observed in rigor and the lowest one in relaxed state (Fig. 6).

Mechanical properties of permeabilized and Triton-treated muscle fibers in relaxed, Ca-activated (pCa 4.2) and rigor states are summarized in Table 1.

Measurements on slightly wet fibers in air gave similar relationships between transverse stiffness values in different regions of the sarcomere and different states of the fiber (Table 2). However, both permeabilized and Triton-treated fibers exhibited much higher transverse stiffness and Young's modulus as compared to fibers in solution.

DISCUSSION

AFM images of the muscle fiber show regular periodic humps of the fiber surface (Figs. 2–4). There are two kinds of structures within a period. One structure is ~1.6 μm long (along the fiber axis), another one is ~0.8 μm. Both

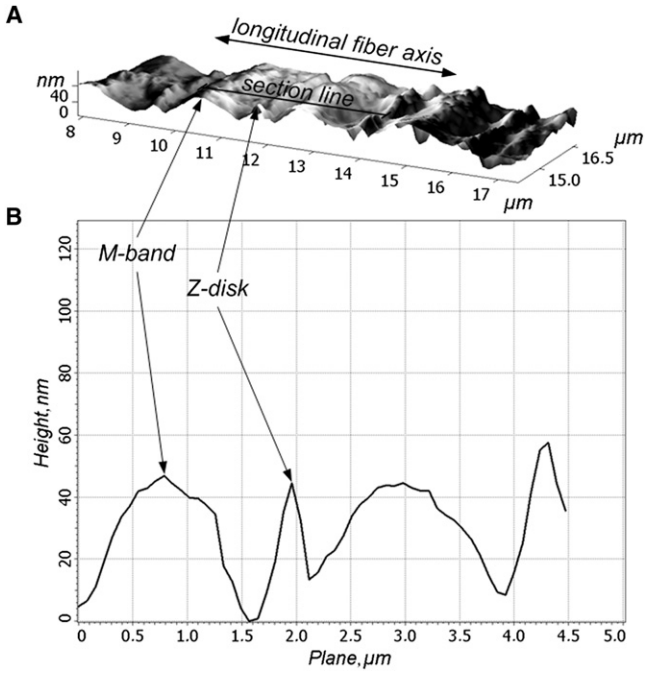

FIGURE 3 Three-dimensional AFM area scan (*A*) and a surface profile (*B*) along a section line of Triton-treated muscle fiber in relaxed state. After Triton X-100 treatment the height of the Z-disk and M-band humps decreases compared to those in Fig. 2.

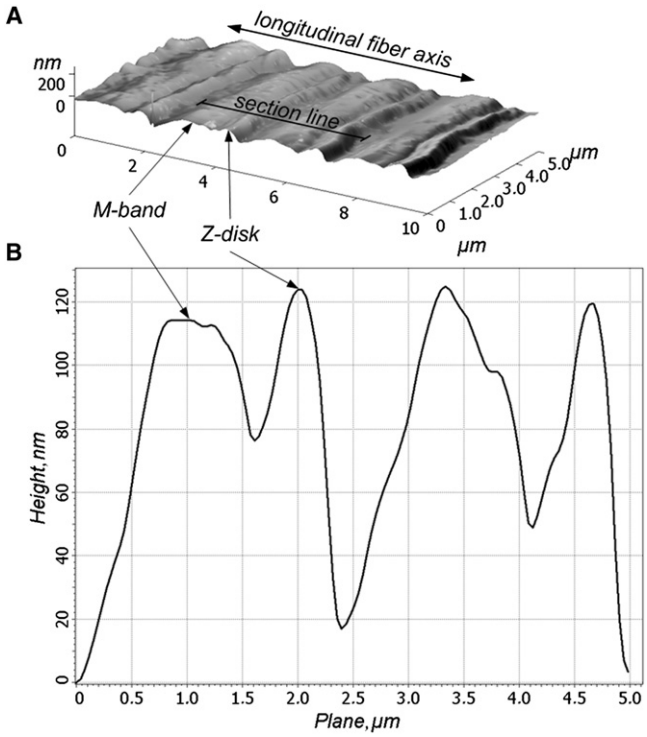

FIGURE 4 Three-dimensional AFM area scan (*A*) and surface profile (*B*) along a section line of a permeabilized muscle fiber from in rigor. In rigor the height of the Z-disk (but not the M-band) humps is increased compared to the relaxed state (see Fig. 2).

structures have a 2.3–2.5 μm period. According to Hodge et al. (16) we attributed that the first structure to the A-band with the M-disk in the middle, and the second one to the I-band with the Z-disk in the middle. Humps in the regions of the M-bands and Z-disks are possibly caused by the presence of transversely-oriented submembrane cytoskeleton structures. Similar results were obtained on skeletal muscle fibers from CD1 mice in solution and in air (7). We have shown the humps in the Z-disk regions of the sarcomeres on the AFM scans and assumed that the humps are due to costameres. To prove our assumption, we used fluorescent antibodies against α-actinin and localized them with AFM and fluorescent microscopy. Our scans are similar to those described in Defranchi et al. (7) so we assume that the structures localized in the Z-disk humps are likely to be costameres formed by extra sarcomeric proteins. The submembrane structure collated near the M-bands may be formed by some proteins, possibly including obskurin (4). However, some uncertainty does remain as to whether our fiber preparation procedures, etc. may have altered the costamere structures.

Using the AFM surface images, we were able to measure transverse stiffness of specific regions of the fiber such as projections of the M-band and Z-disks. As treatment with Triton X-100 destroys sarcolemma and sarcolemma-associated cytoskeleton, comparison of stiffness of permeabilized and Triton-treated fibers allows one to dissect mechanical properties of myofibrils and extra sarcomere cytoskeleton. It should be noted, however, that our preparations have some limitations. Glycerol treatment as well as EGTA treatment results in permeabilization of sarcolemma that is needed for free diffusion of Ca^{2+} and ATP to the fiber. A number of studies of contractile properties of muscle glycerinated fibers have been published (e.g., 17–19). Although this is an established approach, we scanned the fiber surface before stiffness measurement to choose the region where the surface structure was better preserved. Treatment with Triton-X100 allowed us to destroy sarcolemma, but could not guarantee total removal of subsarcolemma cytoskeleton.

Our values for the Young modulus of permeabilized muscle fibers in relaxed state (30.4 $\pm$ 1.8 kPa at the M-band projection, 39 $\pm$ 4 kPa at the Z-disk projection and 22 $\pm$ 3 kPa between them) are close to those reported for the fibers from CD1 mouse (61 $\pm$ 5 kPa (7)) and C2C12 myoblasts from C3H mouse (24.7 $\pm$ 3.5 kPa (6)). However, previous reports did not identify in which regions along the fiber axis the measurements were taken. In our experiments, the regional difference in transversal fiber stiffness was observed in all types of specimens in all three fiber states (Tables 1 and 2). In all regions there was an ~2-fold increase in stiffness on activation with Ca^{2+} and an ~3-fold increase when the fiber was transferred to rigor.

The measurements of transversal stiffness of relaxed Triton-treated fibers yielded the values 8.2 $\pm$ 0.9 pN/nm

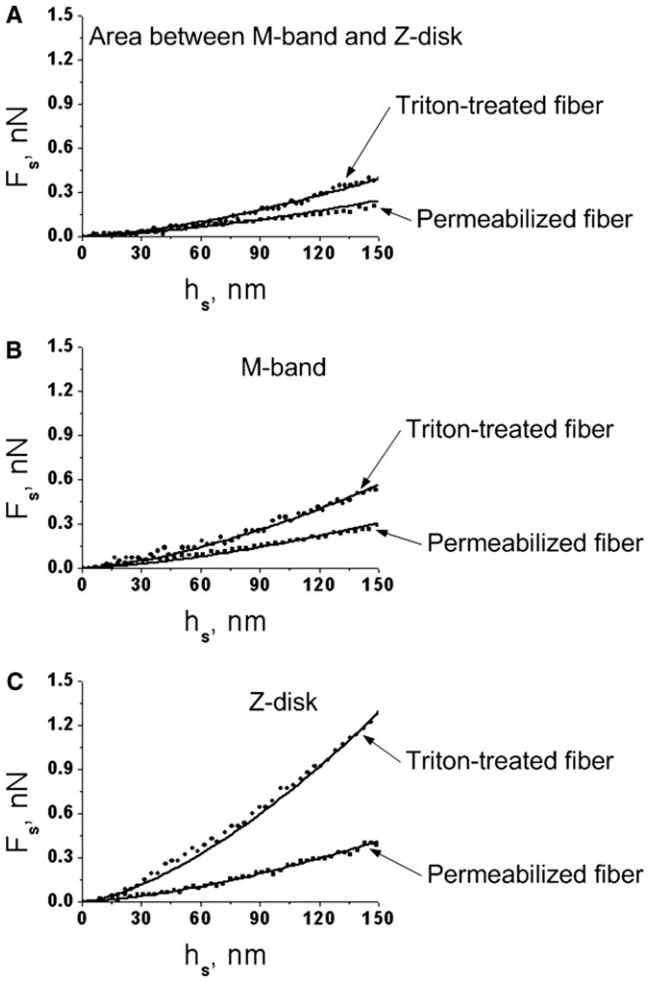

FIGURE 5 Force-distance curves for the muscle fibers in relaxing solution *R*. Squares show experimental data for a permeabilized fiber, circles correspond to a Triton-treated fiber. Lines represent least-square fits of the data to Eq. 1. (*A*) Area between the M-band and Z-disk: transversal stiffness $k_s = 1.37$ pN/nm, Young's modulus $E = 22.7$ kPa for permeabilized fiber, $k_s = 2.07$ pN/nm, $E = 36.5$ kPa for Triton-treated fiber. (*B*) M-band: $k_s = 1.92$ pN/nm, $E = 28.7$ kPa (permeabilized fiber) and $k_s = 3.6$ pN/nm, $E = 52.4$ kPa (Triton-treated fiber). (*C*) Z-disk: $k_s = 2.72$ pN/nm, $E = 38.5$ kPa (permeabilized fiber) and $k_s = 8.2$ pN/nm, $E = 124$ kPa (Triton-treated fiber).

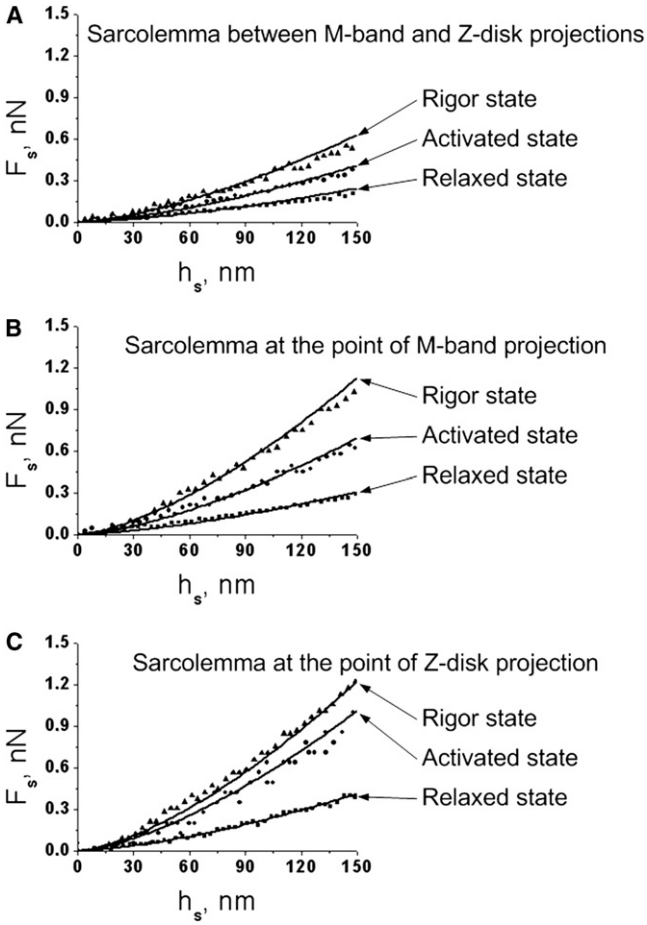

FIGURE 6 Force-distance curves for permeabilized muscle fiber in relaxed (*squares*), Ca-activated (*circles*), and rigor (*triangles*) states. Lines represent least-square fits of the data to Eq. 1. (*A*) Sarcolemma between the M-band and the Z-disk projections: transversal stiffness $k_s = 1.37$, 2.54, 3.64 pN/nm, Young's moduli $E = 22.7$, 38.2, 58.8 kPa, respectively. (*B*) Sarcolemma at the M-band projection: $k_s = 1.92$, 4.16, 6.17 pN/nm, $E = 28.7$, 64.6, 105 kPa. (*C*) Sarcolemma at the Z-disk projection: $k_s = 2.72$, 6.74, 8.2 pN/nm, $E = 38.5$, 94.6, 115 kPa.

for the Z-disk, 3.7 ± 0.3 pN/nm for the M-band, and 2.1 ± 0.2 pN/nm between the Z-disk and M-band. These values are comparable to the stiffness coefficient reported in similar experiments for isolated myofibrils from newborn rats (3 pN/nm (20)) and myofibrillar bundles from *Drosophila* (4.4 ± 2.0 pN/nm (21)). Our data also agree with those of Xu et al. (22), who used osmotic compression to measure transversal stiffness. They found that transversal stiffness of isolated skinned fibers from rabbit m. psoas in rigor is 340 pN/(thick filament × nm). Assuming a spacing of the 1.0 equatorial reflection d_{10} of 39 nm and cross-sectional area of thick filament surrounded by six thin filaments as $2/\sqrt{3}d_{1,0}^2$ one can obtain transversal stiffness of 7.56 pN/nm close to that found here under similar conditions 10.3 ± 2 pN/nm (Table 1). It should be noted, however, that stiffness of Triton-treated fibers does not increase on Ca-activation and rigorization in the same proportion as in permeabilized ones. The Z-disk stiffness increases in 1.5 times on activation and twofold after transferring to rigor. The M-line stiffness changes similarly to that in permeabilized fibers. Changes in stiffness between the M-line and Z-disk were more pronounced (2.5 and 5 times, respectively) (Table 1).

Significant increase in transversal stiffness between the M-bands and Z-disks was possibly caused by myosin cross-bridges between the thin and thick filaments on activation and in rigor. Xu et al. (22) have shown that one of the key parameters of radial elasticity is the equilibrium spacing, whereas the fibers in different states exhibited a broad range of radial stiffness coefficients depending, in the opinion of Xu et al. (22), on the state of the cross-bridges rather than

TABLE 1 Transversal stiffness and Young's modulus of isolated muscle fibers in liquid

	Permeabilized fibers			Triton-treated fibers		
	Transversal stiffness (pN/nm)	Young's modulus (kPa)	Measurements (*n*)	Transversal stiffness (pN/nm)	Young's modulus (kPa)	Measurements (*n*)
Relaxed						
Z	2.5 ± 0.3	39 ± 4	39	8.2 ± 0.9	124 ± 14	61
M	1.9 ± 0.1	30 ± 2	38	3.7 ± 0.3	53 ± 4	33
M–Z	1.4 ± 0.2	22 ± 3	39	2.1 ± 0.3	38 ± 6	31
Activated						
Z	6.3 ± 0.5	97 ± 8	44	11.3 ± 0.2	171 ± 15	60
M	4.1 ± 0.6	66 ± 10	41	6.9 ± 0.4	99 ± 8	31
M–Z	2.3 ± 0.5	38 ± 9	46	5.3 ± 0.6	71 ± 11	34
Rigor						
Z	8.0 ± 0.2	115 ± 3	34	18.0 ± 1.9	272 ± 29	90
M	6.5 ± 0.4	105 ± 3	36	14.5 ± 1.8	219 ± 27	87
M–Z	3.6 ± 1.1	60 ± 8	35	10.3 ± 2	156 ± 29	81

Z and *M* correspond to measurement taken at the Z-disk and M-band projections on the fiber surface.

on the fraction of the myosin heads bound to actin. Ranatunga et al. (19) have shown that isometric tension of muscle fibers in the relaxed state (passive tension) was insensitive to increased pressure, whereas the muscle fiber tension in rigor state increased linearly with pressure. They could not exclude that changes in rigor tension are induced by hydrostatic compression of specific elastic component in a cross-bridge. It is possible that increase in transversal stiffness of the Z-disks and M-bands (Table 1) is probably a second-order effect caused by cross-bridge formation in the overlap zone.

The mechanism of a less pronounced increase in transversal stiffness of different regions of permeabilized fibers remains unclear. A complex nonlinear relation between axial and transversal stiffness was suggested (23). This nonlinearity can explain the difference in amount of increase of transversal stiffness in different regions of the fiber. One can assume that a number of proteins including desmin can be involved in the mechanism of force transduction from the contractile apparatus to sarcolemma.

Such force transduction may be of mechanical importance as it provides fiber integrity under stress and may participate in mechano-signaling and mechano-transduction. Kumar et al. (23) have shown that there are two distinct signaling pathways activated in response to mechanical stress applied axially and transversely to diaphragm muscle fibers. Their data show that PI3K, PKC, and MEK1/2 (family of mitogen-activated protein kinases) are activated when the mechanical stress is applied axially, but not activated when stress is applied transversally. On the other hand, cyclic AMP-dependent PKA is activated only in response to ransverse mechanical stress. Taking into account the data showing changes in transversal stiffness during differentiation (8), one can assume that changes in force transduction from the contractile apparatus to extra sarcomere structures may activate or depress signal pathway to direct differentiation.

The mechanical properties of slightly wet fibers measured in air have yielded generally similar results, showing an increase in the transversal stiffness of the muscle fiber after activation and in rigor. However, the values for the transversal stiffness and Young's modulus of such fibers were about an order of magnitude higher than for the fibers in liquid probably due to drying of the specimens. Although

TABLE 2 Transversal stiffness and Young's modulus of wet muscle fibers in air

	Permeabilized fibers			Triton-treated fibers		
	Transversal stiffness (pN/nm)	Young's modulus (MPa)	Measurements (*n*)	Transversal stiffness (pN/nm)	Young's modulus (MPa)	Measurements (*n*)
Relaxed						
Z	36 ± 3	1.7 ± 0.2	4	81 ± 6	4.5 ± 0.5	35
M	31 ± 3	1.2 ± 0.1	4	59 ± 10	2.9 ± 0.4	24
Activated						
Z	70 ± 4	2.6 ± 0.2	4	110 ± 7	6.2 ± 0.4	25
M	45 ± 8	1.3 ± 0.4	3	92 ± 6	5.15 ± 0.5	9
Rigor						
Z	92 ± 20	5.7 ± 1.0	25	132 ± 16	7.3 ± 0.9	16
M	54 ± 10	2.7 ± 0.5	9	109 ± 5	6.1 ± 0.3	17

Z and *M* correspond to measurement taken at the Z-disk and M-band projections on the fiber surface.

this preparation cannot reproduce mechanical characteristics of muscle fibers in vivo the data illustrate the importance of water balance on fiber mechanics.

We conclude that transversal stiffness of a fiber is maximal at the projections of the Z-disks, lower at the projections of the M-band, and minimal between them. Treatment of fibers with Triton increases their stiffness, but does not affect its regional difference. When actin-myosin cross-bridges are formed on Ca-activation and in rigor, myofibril stiffness increases leading to increase in transversal fiber stiffness. We suspect that such effects may arise from the stress applied from the contractile apparatus to sarcolemma bringing about deformation of the cytoskeleton proteins such as desmin, extra sarcomeric actin, alfa-actinin, and possibly obscurin.

The authors thank Andrey Tsaturyan for very helpful discussions.

This work was supported by the Program of Division of Biological Science RAS "Physiological mechanisms for internal regulation and organization of living systems."

REFERENCES

1. Bloch, R. J., and H. Gonzalez-Serratos. 2003. Lateral force transmission across costameres in skeletal muscle. *Exerc. Sport Sci. Rev.* 31:73–78.
2. Barton, E. R. 2006. Impact of sarcoglycan complex on mechanical signal transduction in murine skeletal muscle. *Am. J. Physiol. Cell Physiol.* 290:C411–C419.
3. Capetanaki, Y., R. J. Bloch, …, S. Psarras. 2007. Muscle intermediate filaments and their links to membranes and membranous organelles. *Exp. Cell Res.* 313:2063–2076.
4. Fukuzawa, A., S. Lange, …, M. Gautel. 2008. Interactions with titin and myomesin target obscurin and obscurin-like 1 to the M-band: implications for hereditary myopathies. *J. Cell Sci.* 121:1841–1851.
5. Puchner, E. M., A. Alexandrovich, …, M. Gautel. 2008. Mechanoenzymatics of titin kinase. *Proc. Natl. Acad. Sci. USA.* 105:13385–13390.
6. Mathur, A. B., A. M. Collinsworth, …, G. A. Truskey. 2001. Endothelial, cardiac muscle and skeletal muscle exhibit different viscous and elastic properties as determined by atomic force microscopy. *J. Biomech.* 34:1545–1553.
7. Defranchi, E., E. Bonaccurso, …, C. Reggiani. 2005. Imaging and elasticity measurements of the sarcolemma of fully differentiated skeletal muscle fibers. *Microsc. Res. Tech.* 67:27–35.
8. Collinsworth, A. M., S. Zhang, …, G. A. Truskey. 2002. Apparent elastic modulus and hysteresis of skeletal muscle cells throughout differentiation. *Am. J. Physiol. Cell Physiol.* 283:C1219–C1227.
9. Stevens, L., Y. Mounier, and X. Holy. 1993. Functional adaptation of different rat skeletal muscles to weightlessness. *Am. J. Physiol.* 264:R770–R776.
10. Walker, S. M., and G. R. Schrodt. 1965. Continuity of the T system with the sarcolemma in rat skeletal muscle fibers. *J. Cell Biol.* 27:671–677.
11. Carl, Ph., and H. Schillers. 2008. Elasticity measurement of living cells with an atomic force microscope: data acquisition and processing. *Pflugers Arch.* 457:551–559.
12. Hertz, H. 1882. Ueber die Beruhrung fester alastischer Korper. *Reine Angew Mathematik.* 92:156–171.
13. Sneddon, I. N. 1965. The relation between load and penetration in the axisymmetric Boussinesq problem for a punch of arbitrary profile. *Int. J. Eng. Sci.* 3:47–57.
14. Radmacher, M., M. Fritz, …, P. K. Hansma. 1996. Measuring the viscoelastic properties of human platelets with the atomic force microscope. *Biophys. J.* 70:556–567.
15. Shin, D., and K. Athanasiou. 1999. Cytoindentation for obtaining cell biomechanical properties. *J. Orthop. Res.* 17:880–890.
16. Hodge, A. J., H. E. Huxley, and D. Spiro. 1954. Electron microscope studies on ultrathin sections of muscle. *J. Exp. Med.* 99:201–206.
17. Borejdo, J., and S. Putnam. 1977. Polarization of fluorescence from single skinned glycerinated rabbit psoas fibers in rigor and relaxation. *Biochim. Biophys. Acta.* 459:578–595.
18. Kaldor, G., W. DiBattista, and L. Nuler. 1982. Comparative studies on the enzymological and contractile properties of glycerinated muscle fibers and actomyosin suspensions. *Physiol. Chem. Phys.* 14:125–128.
19. Ranatunga, K. W., N. S. Fortune, and M. A. Geeves. 1990. Hydrostatic compression in glycerinated rabbit muscle fibers. *Biophys. J.* 58:1401–1410.
20. Akiyama, N., Y. Ohnuki, …, T. Yamada. 2006. Transverse stiffness of myofibrils of skeletal and cardiac muscles studied by atomic force microscopy. *J. Physiol. Sci.* 56:145–151.
21. Nyland, L. R., and D. W. Maughan. 2000. Morphology and transverse stiffness of *Drosophila* myofibrils measured by atomic force microscopy. *Biophys. J.* 78:1490–1497.
22. Xu, S., B. Brenner, and L. C. Yu. 1993. State-dependent radial elasticity of attached cross-bridges in single skinned fibers of rabbit psoas muscle. *J. Physiol.* 465:749–765.
23. Kumar, A., I. Chaudhry, …, A. M. Boriek. 2002. Distinct signaling pathways are activated in response to mechanical stress applied axially and transversely to skeletal muscle fibers. *J. Biol. Chem.* 277:46493–46503.